

Synthesis and crystal structures of dimethylaminoethanol adducts of Ni(II) acetate and Ni(II) acetylacetonate. Precursors for the sol–gel deposition of electrochromic nickel oxide thin films

Paul A. Williams,^a Anthony C. Jones,^{*a,b} Jamie F. Bickley,^a Alexander Steiner,^a Hywel O. Davies,^{*b} Timothy J. Leedham,^b Susan A. Impey,^c Joanne Garcia,^c Stephen Allen,^c Aline Rougier^d and Alexandra Bly^d

^aDepartment of Chemistry, University of Liverpool, Liverpool, UK L69 7ZD.

E-mail: tony@tjconsultancy.demon.co.uk

^bInorgtech Limited, 25 James Carter Road, Mildenhall, Suffolk, UK IP28 7DE.

E-mail: hywel@inorgtech.co.uk

^cSchool of Industrial and Manufacturing Science, University of Cranfield, Cranfield, Bedford, UK MK43 0AL

^dL RCS, Université de Picardie Jules Verne, 33 rue Saint-Leu, 80039 Amiens Cedex, France

Received 12th April 2001, Accepted 11th June 2001

First published as an Advance Article on the web 2nd August 2001

The reaction between *N,N*-dimethylaminoethanol (dmaeH) and nickel(II) acetylacetonate, [Ni(acac)₂]₃ or Ni(II) acetate tetrahydrate, [Ni(CH₃CO₂)₂(H₂O)₄] yields the new complexes [Ni(acac)₂(dmaeH)] (**1**) and [Ni(CH₃CO₂)₂(dmaeH)₂] (**2**). Complexes (**1**) and (**2**) are mononuclear, containing six-coordinate Ni(II) atoms in slightly distorted octahedral environments. Complex (**1**) contains two bidentate and chelating acetylacetonate groups with a chelating dmaeH ligand. Complex (**2**) contains two monodentate acetate groups in a *cis* configuration and two chelating dmaeH ligands. Both complexes dissolve readily in dmaeH to form stable solutions, and are good precursors for the deposition of NiO thin films by sol–gel techniques. (**1**) and (**2**) were successfully used to grow electrochromic NiO thin films on conductive glass substrates. The surface morphology of the films was characterised by scanning electron microscopy (SEM) and atom force microscopy (AFM). The thin film performances were characterised by means of optical (transmittance) and electrochemical (cyclic voltammetry) methods. Upon cycling, the NiO thin films switch from brown to transparent in a reversible way exhibiting anodic electrochromic performance.

1. Introduction

There has been considerable recent interest in the development of chemical routes (*e.g.* sol–gel) for the deposition of nickel oxide (NiO) and complex oxides containing nickel, which have a number of important industrial applications.¹ For instance, nickel oxide is a component of electrochromic devices such as switchable automobile mirrors and smart windows,² whilst nickel ferrite and nickel zinc ferrite find application in high frequency microwave devices.³

Progress in the sol–gel deposition of NiO has been severely restricted by the lack of suitable NiO precursors with sufficient solubility and stability in alcohol solution. Nickel alkoxides [Ni(OR)₂]_{*n*} are polymeric, poorly characterised and are generally insoluble in alcohols at room temperature,⁴ making them unsuitable for sol–gel applications. In an attempt to obtain soluble nickel alkoxide complexes, donor functionalised alkoxide groups, such as dimethylaminoisopropoxide [OCH(Me)CH₂NMe₂] have been utilised, but the resulting product was an inseparable mixture of [Ni(OCH(Me)CH₂NMe₂)₂] and [Li(Pr¹OH)Ni(OCH(Me)CH₂NMe₂)Cl]₂.⁵ Nickel β-diketonatoalkoxides, such as [Ni₄(OMe)₄(β-dik)₄(MeOH)₄] have also been synthesised,⁶ but these are insoluble in alcohols.

Sol–gel nickel oxide films have been successfully deposited from mixtures of nickel nitrate, [Ni(NO₃)₂(H₂O)₆] in alcohol solutions,⁷ but there are serious doubts about the stability of Ni(NO₃)₂ during thermal processing, making the process unattractive for large scale coating applications.

Metal acetates and acetylacetonates have been used as

alternative precursors to metal alkoxides in sol–gel oxide deposition processes,⁸ and our efforts have therefore been directed into obtaining alcohol soluble Ni(II)–acetate and Ni(II)–acetylacetonate complexes. Acetate and β-diketonate derivatives of divalent 3d transition metals such as Ni(II) have a marked tendency to polymerise,⁹ typified by [Ni(acac)₂]₃ which is an acac-bridged trinuclear species.^{10,11} Other trinuclear Ni β-diketonates include [Ni(benzoylacetonate)₂]₃¹² and [Ni(dibenzoylmethanate)₂]₃.¹² The addition of nitrogen donor ligands such as pyridine (py) and piperidine (pip) leads to partial breakdown of the [Ni(acac)₂]₃ trimer to give the binuclear complexes, [Ni(acac)₂(py)]₂¹¹ and [Ni(acac)₂(pip)]₂.¹¹ The mononuclear complexes [Ni(acac)₂(H₂O)₂]₃¹³ and [Ni(CH₃CO₂)₂(H₂O)₄]¹⁴ are known, but both compounds have only a very limited room temperature solubility in alcohols, making them unsuitable for sol–gel applications.

We have now found that the addition of a donor functionalised alcohol such as *N,N*-dimethylaminoethanol, [HOCH₂CH₂NMe₂] (dmaeH), which contains both an oxygen and nitrogen donor function, to [Ni(acac)₂]₃ leads to complete breakdown of the trimer to give the mononuclear complex [Ni(acac)₂(dmaeH)] (**1**). We have also found that the addition of dmaeH to nickel acetate tetrahydrate, [Ni(CH₃CO₂)₂(H₂O)₄] also gives a monomeric Ni(II) complex, [Ni(CH₃CO₂)₂(dmaeH)₂] (**2**). DmaeH has thus proved to be a good dehydrating agent, and this may have further applications in synthesis as few successful dehydrating agents are known for transition metal complexes. Significantly, both (**1**) and (**2**) have reasonable solubility in simple alcohols such as MeOH and EtOH

(ca. 0.1 mol l⁻¹) and are highly soluble in dmaeH, making them suitable for sol-gel applications. In this paper, the synthesis, characterisation and X-ray crystal structures of (1) and (2) are reported and their successful use as precursors for the sol-gel deposition of electrochromic NiO thin films is described. Typical optical/electrochemical performances of sol-gel NiO films are also reported.

2. Experimental

General techniques

All manipulations were performed under dry nitrogen using standard Schlenk flask/vacuum line techniques. *N,N*-Dimethylaminoethanol (dmaeH) (Aldrich) was dried by distillation off potassium hydroxide and stored over molecular sieves. Infrared spectra were recorded on a Perkin Elmer 177 spectrometer using Nujol mulls between NaCl plates. Atom force microscopy (AFM) was carried out using a Digital Instruments NanoScope IIIa scanning probe microscope and scanning electron micrography (SEM) was performed on a Philips XL30 FEG. The structure of the films was examined by X-ray diffraction (XRD) using a Siemens D5005 diffractometer. The optical transmission measurements were performed on a Cary spectrophotometer between 300 and 2000 nm. The electrochemical properties of the films were characterised by cyclic voltammetry performed on an autolab PGSTAT 30 system. Films were cycled at 20 mV s⁻¹ in 0.1 M KOH solution with a standard three electrode configuration consisting of the sample (working electrode), a conventional saturated calomel electrode (SCE) immersed in saturated KCl solution (reference electrode), and a high purity platinum mesh (counter electrode).

Precursor synthesis

Ni(II) acetylacetonate, [Ni(acac)₂]₃ and Ni(II) acetate tetrahydrate, [Ni(CH₃CO₂)₂(H₂O)₄] were synthesised by literature methods^{15,16} from mixtures of [NiCl₂(H₂O)₆] and acacH or CH₃CO₂H, respectively.

[Ni(acac)₂(dmaeH)] (1)

[Ni(acac)₂]₃ (7.89 g, 10.2 mmol) was dissolved in hot toluene (120 cm³) with stirring to give a dark green solution. An excess of dmaeH (20 cm³, 199 mmol) was then carefully added. The solution was then heated to reflux and maintained at this temperature for 4 hours. The dark green solution was filtered hot and allowed to cool to room temperature. The volume of the solvent was reduced *in vacuo* (to ca. 75%) and the resulting solution was left to stand at room temperature overnight to give compound (1) as air-sensitive dark green crystals (mp 180–185 °C). Yield: 1.45 g, 14% (based on [Ni(acac)₂]₃).

Anal. Calc. for C₁₄H₂₅O₅NNi: C, 48.7; H, 7.3; N, 4.1%. Found: C, 48.7; H, 7.5; N, 4.1%.

IR (Nujol, cm⁻¹): 1608(s), 1516(s), 1412(s), 1327(m), 1253(m), 1195(w), 1170(w), 1099(vw), 1073(m), 1017(m), 948(w), 920(m), 885(w), 783(vw), 762(w), 756(vw), 750(m), 722(w), 654(w).

[Ni(CH₃CO₂)₂(dmaeH)₂] (2)

[Ni(CH₃CO₂)₂(H₂O)₄] (10 g, 50 mmol) was added to dmaeH (50 cm³) and the mixture was heated to reflux for 1 h to give a dark green solution. The mixture was then allowed to cool and was stored at room temperature overnight. Compound (2) was obtained as air-sensitive dark green crystals. Yield 9.2 g, 58% (based on [Ni(CH₃CO₂)₂(H₂O)₄]).

Anal. Calc. for C₁₂H₂₈O₆N₂Ni: C, 40.60; H, 7.95; N, 7.89%. Found: C, 40.93; H, 8.07; N, 7.88%.

IR (Nujol, cm⁻¹): 2046(w), 1981(w), 1542(s), 1414(s),

1349(w), 1332(w), 1275(w), 1259(w), 1181(vw), 1168(vw), 1096(w), 1059(s), 1028(w), 950(m), 914(w), 880(w), 784(w), 722(vw), 665(m), 618(w).

Single crystal X-ray diffraction

Single crystals of (1) and (2) suitable for X-ray diffraction were obtained directly from the reaction mixtures by filtration. The complexes had a marked tendency to decompose, presumably by loss of adducted dmaeH, and were thus handled under nitrogen throughout. Crystallographic data were recorded on a Stoe-IPDS diffractometer using graphite monochromated Mo-K_α radiation (λ = 0.71073 Å), T = 200 K. Structures were solved by Direct Methods and refined by full-matrix least squares against F² using all data.¹⁷ Crystal and data collection parameters are given in Table 1.

CCDC reference numbers 156618 and 156619. See <http://www.rsc.org/suppdata/jm/b1/b103288g/> for crystallographic data in CIF or other electronic format.

Sol-gel deposition of NiO

All processes were carried out in a class 1000 clean room. Indium tin oxide (ITO) coated glass substrates (typically 30 × 30 × 0.7 mm) were very carefully cleaned by vapour degreasing with Analytical Grade isopropyl alcohol.

Precursor solutions of (1) and (2) in dry dmaeH (0.05–0.5 M) were filtered (0.2 μm) and subsequently deposited on preheated (60 °C) glass on the conductive side of the substrates. The substrates were then spun between 1000 and 4000 rpm on a photo resist spinner (model 400, Electronic Micro Systems). Large glass panels (300 × 300 × 0.7 mm) were spun at 1000 rpm on a large home built whirler.

The coatings were left to dry in air for 5 min at room temperature (20 °C) and then at 100 °C for 20 min on a hotplate. The samples were then fired on a hotplate at 200 °C for 60 min. Uniform NiO thin films were obtained, with the colour depending on the thickness obtained. The surface morphology of the films was examined by AFM and SEM. The electro-optical performances of the films were tested.

3. Results and discussion

Crystal structures of complexes (1) and (2)

The molecular structure of complex (1) is shown in Fig. 1, and important bond lengths and angles are summarised in Table 2. The complex is mononuclear with distorted octahedral geometry around the Ni(II) atom and contains two bidentate/chelating acac groups in a planar configuration and a bidentate

Table 1 Crystal and data collection parameters for [Ni(acac)₂(dmaeH)] (1) and [Ni(OAc)₂(dmaeH)₂] (2)

	1	2
Chemical formula	C ₁₄ H ₂₅ O ₅ NNi	C ₁₂ H ₂₈ O ₆ N ₂ Ni
Formula weight	346.11	355.13
Crystal system	Triclinic	Triclinic
Space group	P $\bar{1}$	P $\bar{1}$
Z	2	2
a/Å	7.737(8)	8.2993(14)
b/Å	10.309(7)	8.5256(14)
c/Å	11.812(8)	13.017(2)
α/°	105.97(8)	95.917(19)
β/°	104.33(11)	95.92(2)
γ/°	97.56(11)	109.469(19)
V/Å ³	857.2(12)	854.4(2)
Absorption coefficient/mm ⁻¹	1.088	1.097
Refl. collected	5380	5492
Refl. unique (R _{int})	2519 (0.0851)	2544 (0.0455)
R1 [I > 2σ(I)]	0.0463	0.0332
wR2 (all data)	0.1141	0.0755

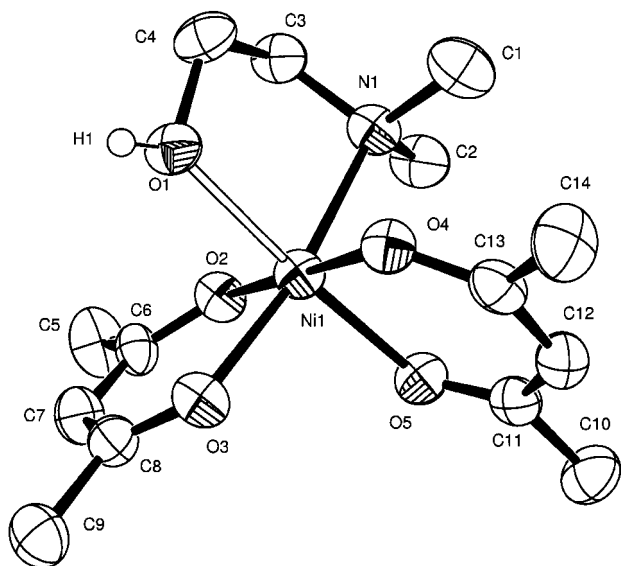


Fig. 1 Crystal structure of $[\text{Ni}(\text{acac})_2(\text{dmaeH})]$ (**1**).

Table 2 Selected bond distances (Å) and angles (°) for $[\text{Ni}(\text{acac})_2(\text{dmaeH})]$ (**1**)

Ni(1)–O(2)	2.026(3)	O(2)–Ni(1)–O(3)	90.65(14)
Ni(1)–O(3)	2.024(4)	O(2)–Ni(1)–O(1)	88.30(16)
Ni(1)–O(4)	2.2045(3)	O(2)–Ni(1)–O(5)	91.33(16)
Ni(1)–O(5)	2.013(4)	O(4)–Ni(1)–O(5)	89.65(16)
Ni(1)–O(1)	2.111(4)	O(4)–Ni(1)–O(1)	90.74(16)
Ni(1)–N(1)	2.169(4)	O(4)–Ni(1)–O(3)	88.87(14)
		O(1)–Ni(1)–O(3)	89.69(15)
		O(3)–Ni(1)–O(5)	95.01(15)
C(6)–O(2)	1.262(6)	O(2)–Ni(1)–O(4)	178.94(13)
C(8)–O(3)	1.258(6)	O(5)–Ni(1)–O(1)	175.27(13)
C(11)–O(5)	1.250(6)		
C(13)–O(4)	1.285(6)	O(4)–Ni(1)–N(1)	92.24(14)
		O(2)–Ni(1)–N(1)	88.07(15)
		O(5)–Ni(1)–N(1)	95.04(16)
		O(3)–Ni(1)–N(1)	169.90(13)
		N(1)–Ni(1)–O(1)	80.31(14)

chelating dmaeH ligand. As in the case of the related complex $[\text{Ni}(\text{acac})_2(\text{H}_2\text{O})_2]$,¹³ there is no evidence for tetragonal distortion with the major distortions being O(3)–Ni(1)–N(1) at 169.90(13)° and O(1)–Ni(1)–N(1) at 80.31(14)°. Two $[\text{Ni}(\text{acac})_2(\text{dmaeH})]$ moieties are loosely associated *via* hydrogen bonding from O(1)H on one molecule to O(4)[acac] of a neighbouring molecule (see Fig. 2). Six-coordinate Ni(II) atoms invariably display octahedral configuration,¹⁸ such as in the Ni

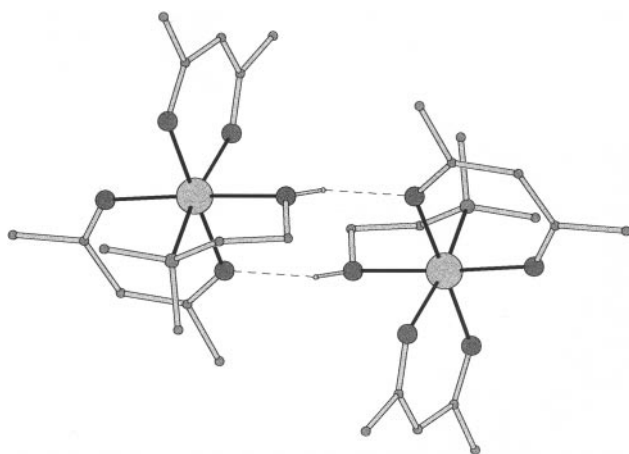


Fig. 2 Intermolecular association between two $[\text{Ni}(\text{acac})_2(\text{dmaeH})]$ units.

β -diketonate complexes, $[\text{Ni}(\text{acac})_2(\text{H}_2\text{O})_2]$,¹³ $[\text{Ni}(\text{acac})_2]_3$,¹¹ $[\text{Ni}(\text{acac})_2(\text{py})]_2$,¹¹ $[\text{Ni}(\text{acac})_2(\text{pip})]_2$,¹¹ and in the adduct complex $[\text{cis-NiCl}_2(\text{HOCH}(\text{Me})\text{CH}_2\text{NMe}_2)_2]$.⁵

Only a few $[\text{Ni}(\text{acac})_2]$ complexes have been structurally characterised, and the only other reported mononuclear complex is $[\text{Ni}(\text{acac})_2(\text{H}_2\text{O})_2]$.¹³ The Ni–O(acac) bond lengths in (**1**) lie in the range 2.013(4)–2.2045(3) Å, very close to the average value of 2.015 Å found in $[\text{Ni}(\text{acac})_2(\text{H}_2\text{O})_2]$.¹³ The Ni–O(acac) bond lengths in (**1**) are in general slightly longer than the Ni–O bond lengths of the terminal acac ligands in $[\text{Ni}(\text{acac})_2]_3$ which lie in the range 1.93(3)–2.00(3) Å.¹¹ The Ni–O bond lengths in (**1**) are also slightly longer than the Ni–O bond lengths of the terminal acac ligands in $[\text{Ni}(\text{acac})_2(\text{py})]_2$ (1.968(17), 2.008(14) Å),¹¹ but are close to the Ni–O bond lengths of the terminal acac group in $[\text{Ni}(\text{acac})_2(\text{pip})]_2$ (2.050(10), 2.033(10) Å).¹¹ The Ni–O(acac) bond lengths in (**1**) are also significantly greater than in the $[\text{Ni}(\text{acac})(\text{dppe})]^+$ cation (1.861(6) Å).¹² It has previously been observed¹⁹ that the mean Ni–O(acac) bond length in the octahedral Ni-acetylacetonate complexes $[\text{Ni}(\text{acac})_2(\text{H}_2\text{O})_2]$ and $[\text{Ni}(\text{acac})_2]_3$ (2.01(7) and 2.015(1) Å) are significantly longer than the Ni–O bond in the tetrahedral complex $[\text{Ni}(\text{thd})_2]$ (thd = 2,2,6,6-tetramethylheptane-3,5-dionate) (1.836(5) Å)¹⁹ and the present work confirms this trend. The effect has been attributed to the presence of electrons in the d orbital of the octahedral complexes which are σ -antibonding with respect to the Ni–O bonds, leading to a lengthening of the bond.

Not surprisingly, the Ni–O bond of the adducting dmaeH ligand is longer (2.111(4) Å) than the Ni–O(acac) bonds (av. 2.027(4) Å), and the longest bond in the complex is the Ni–N bond at 2.169(4) Å. The C–O bond lengths vary in the range 1.125–1.285 Å and are comparable to the C–O bond lengths of 1.282(10) and 1.272° reported in $[\text{Ni}(\text{acac})(\text{dppe})]^+$ ¹² and $[\text{Ni}(\text{acac})_2(\text{H}_2\text{O})_2]$,¹³ respectively.

The Ni–O(dmaeH) bond length of 2.111(4) is very close to the Ni–O(dmaeH) bond distances in the $[\text{cis-NiCl}_2(\text{HOCH}(\text{Me})\text{CH}_2\text{NMe}_2)_2]$ adduct (Ni–O 2.171(7), 2.147(8) Å),⁵ but the Ni–N bond distance in (**1**) (2.169(4) Å) is significantly longer than those in $[\text{cis-NiCl}_2(\text{HOCH}(\text{Me})\text{CH}_2\text{NMe}_2)_2]$ (2.142(9), 2.148(9) Å).

The axial/equatorial O–Ni–O bond angles in (**1**) are close to the ideal octahedral angle of 90°, lying in the range 88.87(14)–95.01(15)°, whilst the axial/axial O–Ni–O angle at 178.94(13)° is very close to the ideal angle of 180°. However, the O–Ni–N bond (169.9(13)°) shows a significant deviation from 180°. The “bite” angles of the two acac groups, O(4)–Ni(1)–O(5) and O(3)–Ni(1)–O(2) (89.65(16) and 90.65(14)°) are close to the ideal octahedral angle of 90°, and are slightly smaller than the average bite angle of 92.4° in $[\text{Ni}(\text{acac})_2(\text{H}_2\text{O})_2]$.¹³ The “bite” angle of the dmaeH adducting ligand, O(1)–Ni(1)–N(1), is significantly less at 80.31(14)° and this is closely comparable to the bite angles of the dmaeH adducting ligands in $[\text{cis-NiCl}_2(\text{HOCH}(\text{Me})\text{CH}_2\text{NMe}_2)_2]$ (80.1(3) and 78.5(3)°).⁵

The molecular structure of (**2**) is shown in Fig. 3, whilst selected bond lengths and angles are given in Table 3. The complex is also mononuclear with distorted octahedral geometry about the Ni(II) centre, and contains two monodentate acetate groups in the *cis*-configuration and two bidentate/chelating dmaeH groups. Tetragonal distortion is not observed, with the major distortions being O(4)–Ni(1)–O(2) (172.91(9)°) and O(1)–Ni(1)–N(1) (82.76(9)°). Two intramolecular hydrogen bonds link the hydroxy function of each dmaeH group with the non-coordinated oxygen atoms of the acetate groups (O(1)–H(1)⋯O(3) = 2.554(3) Å; O(2)–H(2)⋯O(6) = 2.536(3) Å) (see Fig. 3).

Other octahedral Ni(II) complexes containing monodentate acetate groups include nickel acetate tetrahydrate, $[\text{Ni}(\text{CH}_3\text{CO}_2)_2(\text{H}_2\text{O})_4]$ ¹⁴ and bis(acetato)bis(pyridine-2-amidoxime-*N,N'*)-nickel(II)-ethanol(1/2), $[\text{Ni}(\text{CH}_3\text{CO}_2)_2(\text{C}_6\text{H}_7\text{N}_3\text{O}_2)(\text{EtOH})]_2$.²⁰ Monodentate and bridging acetate groups predominate in

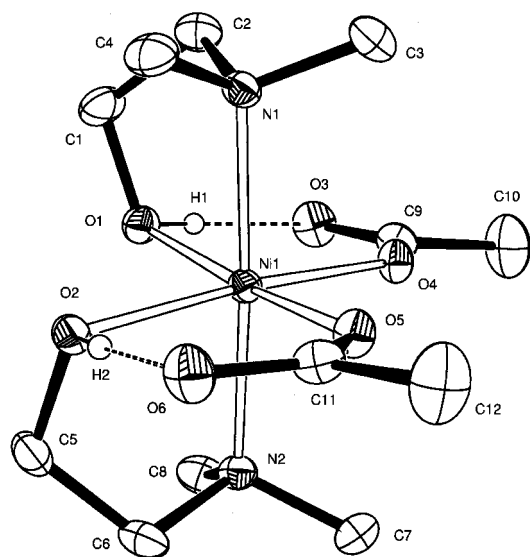


Fig. 3 Crystal structure of $[\text{Ni}(\text{CH}_3\text{CO}_2)_2(\text{dmaeH})_2]$ (**2**).

Table 3 Selected bond distances and angles for $[\text{Ni}(\text{CH}_3\text{CO}_2)_2(\text{dmaeH})_2]$ (**2**)

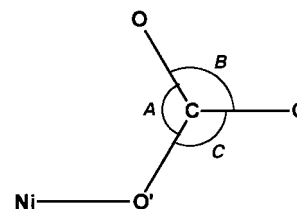
Ni(1)–O(4)	2.050(2)	O(2)–Ni(1)–O(5)	90.63(8)
Ni(1)–O(5)	2.043(2)	O(2)–Ni(1)–O(1)	87.64(8)
Ni(1)–O(1)	2.111(2)	O(4)–Ni(1)–O(5)	91.87(8)
Ni(1)–O(2)	2.109(2)	O(4)–Ni(1)–O(1)	90.64(8)
Ni(1)–N(1)	2.142(3)	O(4)–Ni(1)–O(2)	172.91(9)
Ni(1)–N(2)	2.145(3)	O(1)–Ni(1)–O(5)	173.01(9)
C(11)–O(5)	1.263(4)	O(1)–Ni(1)–N(1)	82.76(9)
C(11)–O(6)	1.260(4)	O(1)–Ni(1)–N(2)	94.72(9)
C(9)–O(3)	1.249(4)	O(5)–Ni(1)–N(2)	91.78(9)
C(9)–O(4)	1.263(4)	O(5)–Ni(1)–N(1)	90.64(9)
C(9)–C(10)	1.504(5)	O(2)–Ni(1)–N(1)	94.69(9)
C(11)–C(12)	1.498(5)	O(2)–Ni(1)–N(2)	82.91(9)
		O(4)–Ni(1)–N(1)	91.91(9)
		O(4)–Ni(1)–N(2)	90.38(9)
		N(2)–Ni(1)–N(1)	176.61(10)
		O(5)–C(11)–O(6)	124.6(3)
		O(4)–C(9)–O(3)	125.7(3)
		O(6)–C(11)–C(12)	118.0(3)
		O(3)–C(9)–C(10)	117.7(3)
		O(5)–C(11)–C(12)	117.4(3)
		O(4)–C(9)–C(10)	116.6(3)

complexes of the late transition metals, although a few examples containing bidentate/chelating acetate groups are known, such as (acetato-*O,O'*)[tris(2-aminoethyl-*N,N',N'',N'''*-nickel(II) perchlorate, $[\text{Ni}(\text{CH}_3\text{CO}_2)_2(\text{C}_6\text{H}_{18}\text{N}_4)](\text{ClO}_4)$.²¹

The Ni–O(acetate) bond lengths in (**2**) of 2.050(2) and 2.043(2) Å are similar to the Ni–O(acac) bond lengths in complex (**1**) and also to those in $[\text{Ni}(\text{CH}_3\text{CO}_2)_2(\text{H}_2\text{O})_4]$ (2.067(3) Å),¹⁴ but are slightly shorter than the Ni–O(acetate) bond in $[\text{Ni}(\text{CH}_3\text{CO}_2)_2(\text{C}_6\text{H}_7\text{N}_3\text{O}_2)(\text{EtOH})_2]$ (2.118(2) Å).²⁰ The Ni–O(dmaeH) bond lengths in (**2**) (2.111(2), 2.109(2) Å) are greater than the Ni–O(acetate) bond lengths and are very close to those in (**1**) and also $[\text{cis-NiCl}_2(\text{HOCH}(\text{Me})\text{CH}_2\text{NMe}_2)_2]$.⁵ The Ni–N bond distances in (**2**) of 2.142(3) and 2.145(3) Å are less than that in (**1**) (2.169(4) Å), but very close

Table 4 Geometry of monodentate acetate groups in octahedral Ni(II) complexes

Complex	C–O/Å	C–O'/Å	C–C/Å	A/°	B/°	C/°	Reference
$[\text{Ni}(\text{CH}_3\text{CO}_2)_2(\text{dmaeH})_2]$	1.260(4), 1.249(4)	1.263(4)	1.498(5), 1.504(5)	124.6(3) 125.7(3)	118.0(3) 117.7(3)	117.4(3) 116.6(3)	This work
$[\text{Ni}(\text{CH}_3\text{CO}_2)_2(\text{H}_2\text{O})_4]$	1.255(5)	1.272(5)	1.503(3)	122.5	119.5	117.9	14
$[\text{Ni}(\text{CH}_3\text{CO}_2)_2(\text{C}_6\text{H}_7\text{N}_3\text{O}_2)(\text{EtOH})_4]$	1.255(4)	1.265(4)	1.511(5)	124.7(3)	117.3(3)	117.9(3)	20



Scheme 1 Geometry of the monodentate acetate group.

to the Ni–N bond distances in $[\text{cis-NiCl}_2(\text{HOCH}(\text{Me})\text{CH}_2\text{NMe}_2)_2]$ (2.1423(9), 2.148(9) Å).⁵

The geometry of a monodentate acetate group is shown in Scheme 1. It has been proposed²² that in a fully ionised $[\text{CH}_3\text{CO}_2^-]$ group the C–O bonds should subtend an angle of 115.7° with the C–C bond, and that the O–C–O angle should be 126° .

The bond lengths and angles in the monodentate acetate group in complex (**1**) are given in Table 4, where they are compared with those in the monodentate acetate groups in $[\text{Ni}(\text{CH}_3\text{CO}_2)_2(\text{H}_2\text{O})_4]$ and $[\text{Ni}(\text{CH}_3\text{CO}_2)_2(\text{C}_6\text{H}_7\text{N}_3\text{O}_2)(\text{EtOH})_2]$. The C–O and O–C–O angles in all three complexes are very similar, and indicate that in all three complexes the monodentate acetate groups are close to being fully ionised.

The O–Ni–O octahedral bond angles of the NiO_4N_2 octahedral core are close to the octahedral angle of 90° , lying in the range $87.64(8)$ – $91.87(8)^\circ$, however the O–Ni–N bond angles show a larger deviation ($82.76(9)$ – $94.69(9)^\circ$), with the internal “bite angles” of the dmaeH ligands ($82.76(9)$, $82.91(9)^\circ$) showing the greatest deviation from 90° . These dmaeH bite angles are slightly larger than those in (**1**) ($80.31(14)^\circ$) and in $[\text{cis-NiCl}_2(\text{HOCH}(\text{Me})\text{CH}_2\text{NMe}_2)_2]$ ($80.1(3)$, $78.5(3)^\circ$).⁵

Sol-gel deposition of NiO

Very thorough cleaning of the glass substrates is crucial to producing successful sol-gel films. Sol viscosities of 3.9 to 8.57 cP were determined for the concentration range (0.05–0.5 M) for sol (**1**) in dmaeH. At low concentrations (0.05 M) of (**1**) or (**2**) in dmaeH, the resulting NiO films are too thin for performance testing. Precursor concentrations of 0.25–0.5 M give a reasonable film thickness. For example, a 0.25 M sol of (**1**) (viscosity = 5.5 cP) and a 0.25 M sol of (**2**) (viscosity = 4.0 cP) spun at 1000 rpm gives optically good quality NiO films (50–70 nm) for both sols. More concentrated sols of (**1**) and (**2**) result in increased film thickness.

X-Ray diffraction study shows that the NiO films deposited by spin-coating using solutions of (**1**) and (**2**) in dmaeH are amorphous (except for the X-ray lines characteristic of the ITO substrate) implying a high degree of amorphisation. However, analysis by selected area electron diffraction (SAED) confirmed that the films were NiO, with the SAED pattern consisting of diffuse rings which could successfully be indexed as cubic NiO. The structure and electrochromic behaviour (discussed below) of the sol-gel films are found to be very similar to performances of sputtered NiO films deposited during this research but not reported here.

AFM images of 2 layer NiO films are shown in Figs. 4 and 5. They are respectively a 140 nm thick film grown from precursor (**1**) and a 110 nm thick film grown from precursor (**2**). Both

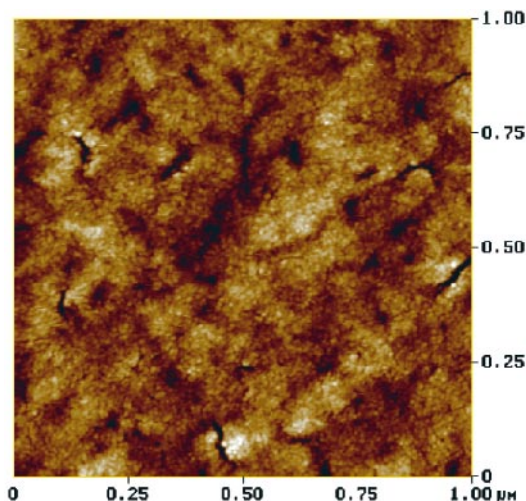


Fig. 4 AFM image of a spun film from a 0.25 M sol of (1) in dmaeH.

images are similar in terms of the underlying particle size, however small surface cracks are observed in the film grown from precursor (1). It is thought likely, but not proven, that the cracks are beneficial for film cycling and also beneficial to the electrochromic performance, as more sites are available for rapid ion exchange. Both films are uniform and smooth with average surface roughness (<1 nm), below that of the ITO substrate (3 nm).

The electro-optical properties of the NiO films were investigated. A typical cyclic voltammogram is shown in Fig. 6. The voltammograms change with the number of cycles suggesting that the film nature and morphology are probably modified in the cycled films compared to the as-deposited system. Indeed, an increase in cathodic and anodic current is seen showing that the number of species that are being oxidised or reduced increases with time. This increase in capacity correlates with an increase in electrochromic properties (discussed below). Upon cycling the films, slightly coloured as deposited, switch from brownish to transparent reversibly. The brown colouration of the film is associated with the oxidation peak prior to current application due to oxygen evolution whereas the bleaching process is associated with the reduction peak.

The electrochromic properties of the films coloured/bleached at step potentials were measured after the sample had been subjected to 10 and 50 cycles in KOH. The samples were coloured by applying step voltages of 0.5 V (vs. SCE) for colouration and 0.0 V for bleaching. The total contrast ratio

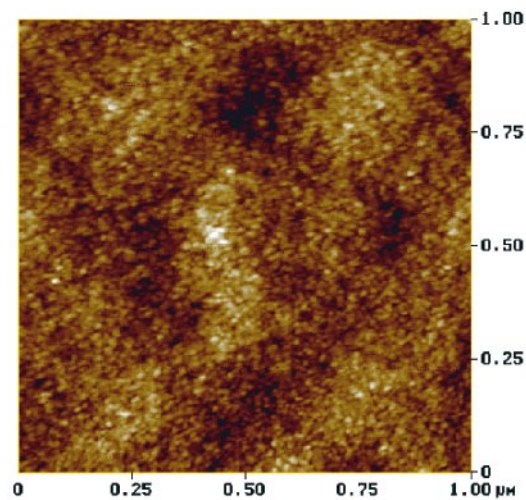


Fig. 5 AFM image of a spun film from a 0.25 M sol of (2) in dmaeH.

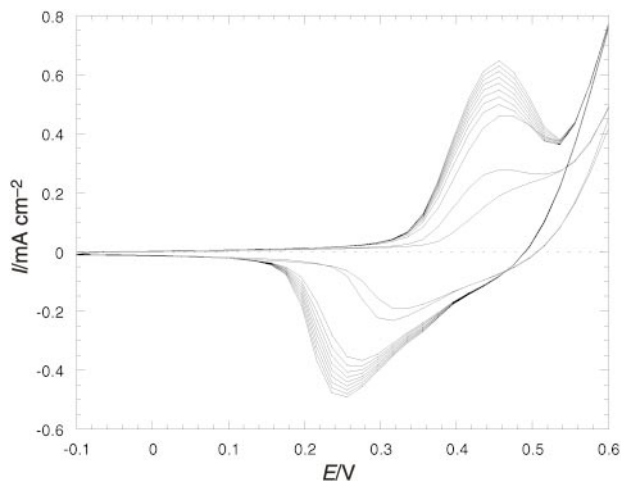


Fig. 6 Voltammograms of Pt/KOH 0.1 M/NiO cells prepared from a 0.25 M solution of (1) in dmaeH. The cell was cycled with a sweep rate of 20 mV s^{-1} .

Table 5 The contrast T_b/T_c and colouration efficiency (CE) with the number of cycles for sol-gel NiO films prepared from a 0.25 M sol of (1) in dmaeH

CE/cm ² C ⁻¹	Number of cycles	Contrast T_b/T_c
13.5	10	1.9
27	50	2.4

T_b/T_c (transmittance in the bleached state/transmittance in the coloured state) is reported in Table 5. As a general comment, the range of optical modulation for the sol-gel films is relatively narrow at very early cycling ($T_b/T_c = 1.9$ after 10 cycles) and increases upon further cycling ($T_b/T_c = 2.4$ after 50 cycles). The colouration efficiency (CE) at 550 nm, expressed as the ratio between the contrast in the bleached state and the coloured state and the charge density (Q), ($CE = (1/Q)\log(T_b/T_c)$) follows a similar trend as values of 13.5 and $27 \text{ cm}^2 \text{ C}^{-1}$ are obtained after 10 and 50 cycles, respectively. The latter value is sufficient for electrochromic devices using tungsten oxides as cathodic electrochromic materials.

4. Conclusions

A simple method has been found for obtaining alcohol-soluble Ni(II) complexes which are suitable for sol-gel applications. Addition of the donor-functionalised alcohol, *N,N*-dimethylaminoethanol (dmaeH) to $[\text{Ni}(\text{acac})_2]_3$ or $[\text{Ni}(\text{CH}_3\text{CO}_2)_2(\text{H}_2\text{O})_4]$ gives the mononuclear octahedral complexes $[\text{Ni}(\text{acac})_2(\text{dmaeH})]$ and $[\text{Ni}(\text{CH}_3\text{CO}_2)_2(\text{dmaeH})_2]$, both of which are highly soluble in dmaeH at room temperature. Both (1) and (2) are excellent precursors for the sol-gel deposition of nickel oxide. The colouration efficiency (determined at 550 nm by cycling) is suitable for electrochromic devices using tungsten oxides as cathodic electrochromic materials.

Acknowledgements

The work was supported by the European Community (Brite Euram III, LANDSEC Project). Cranfield University thanks Christine Kimpton for the AFM images. X. Fanton, F. Beteille and R. Fix from Saint Gobain Recherche, Aubervilliers, Paris, are thanked for helpful discussions.

References

- 1 Y. Ozaki, in *Advanced Ceramics*, ed. S. Saito, Oxford University Press, 1988, ch. 9 and references therein.
- 2 N. Ozer and C. M. Lampert, *Sol. Energy Mater. Sol. Cells*, 1998, **54**, 147.
- 3 J. D. Adam, S. V. Krishnaswamy, S. H. Talisu and K. C. Yoo, *Magn. Mater.*, 1990, **83**, 419.
- 4 R. C. Mehrotra, *Adv. Inorg. Chem. Radiochem.*, 1989, **26**, 269.
- 5 L. G. Hubert-Pfalzgraf, V. G. Kessler and J. Vaissermann, *Polyhedron*, 1997, **16**, 4197.
- 6 M. A. Halrow, J. S. Sun, J. C. Huffman and G. Christou, *Inorg. Chem.*, 1995, **34**, 4167.
- 7 F. H. Moser and N. R. Lynam, *US Pat.*, 4,959,247, 1990.
- 8 N. Ya Turova and M. I. Yanovskaya, in *Ferroelectric Thin Films: Synthesis and Properties*, ed. C. Paz de Araujo, J. C. Scott and G. W. Taylor, Gordon and Breach, Amsterdam, 1996, ch. 8, and references therein.
- 9 J. P. Fackler, *Progr. Inorg. Chem.*, 1966, **7**, 361.
- 10 G. J. Bullen, R. Mason and P. Pauling, *Inorg. Chem.*, 1965, **4**, 456.
- 11 M. B. Hursthouse, M. A. Laffey, P. T. Moore, D. B. New, P. R. Raithby and P. Thornton, *J. Chem. Soc., Dalton Trans.*, 1982, 307.
- 12 G. Favero, B. Coran, M. Basato and S. Issa, *Inorg. Chim. Acta*, 1986, **122**, 129.
- 13 H. Montgomery and E. C. Lingafelter, *Acta Crystallogr.*, 1964, **17**, 1481.
- 14 T. C. Downie, W. Harrison, E. S. Raper and M. A. Raper, *Acta Crystallogr., Sect. B*, 1971, **27**, 706.
- 15 J. N. Van Niekerk and F. R. L. Schoening, *Acta Crystallogr.*, 1953, **6**, 609.
- 16 R. G. Charles and M. A. Pawlikowski, *J. Phys. Chem.*, 1958, **62**, 440.
- 17 G. M. Sheldrick, SHELX 97, Programs for Crystal Structure Solution and Refinement, University of Göttingen, 1997.
- 18 F. A. Cotton and G. Wilkinson, *Advanced Inorganic Chemistry*, John Wiley & Sons Inc., New York, 1988, ch. 18 and references therein.
- 19 F. A. Cotton and J. J. Wise, *Inorg. Chem.*, 1966, **5**, 1200.
- 20 M. Werner, J. Berner and P. G. Jones, *Acta Crystallogr., Sect. C*, 1996, **52**, 72.
- 21 H.-K. Fun, B.-C. Yip, Z.-L. Lu, C. Y. Duan, Y.-P. Tian and X.-Z. You, *Acta Crystallogr., Sect. C*, 1996, **52**, 509.
- 22 T. Hahn, *Z. Kristallogr.*, 1957, **109**, 438.